J Gastroenterol (2011) 46:222–231
DOI 10.1007/s00535-010-0296-3

ORIGINAL ARTICLE—LIVER, PANCREAS, AND BILIARY TRACT

Overexpression of apelin receptor (APJ/AGTRL1) on hepatic stellate cells and sinusoidal angiogenesis in human cirrhotic liver

Hiroaki Yokomori · Masaya Oda · Kazunori Yoshimura · Sanae Machida · Fumihiko Kaneko · Toshifumi Hibi

Received: 28 February 2010 / Accepted: 8 July 2010 / Published online: 20 August 2010

Abstract
Background The apelin receptor (APJ) is related to angiotensin-like-receptor 1 (AGTRL1). This study was designed to elucidate the in vivo localization and changes of APJ in cirrhotic liver, and the in vitro changes of APJ expression in cultured hepatic stellate cells (HSCs) and capillarized sinusoidal endothelial cells (SECs) activated by growth factors.
Methods In vivo studies used control liver samples, cirrhotic liver samples from patients with Child's A cirrhosis undergoing surgical resection (Child-A-LC), and cirrhotic liver samples from autopsied cases of decompensated Child's C cirrhosis (Child-C-LC). Immunohistochemical (IHC), Western blot, laser-capture microdissection (LCM) coupled with reverse transcription -polymerase chain reaction (RT-PCR), and immunoelectron microscopic (IEM) studies for APJ expression were conducted. In vitro examinations used commercial human HSCs and SECs. APJ expression was examined in cultured HSCs activated by growth factors and in capillarized SECs activated by angiogenic factors.
Results The IHC study of liver samples revealed only slight APJ expression in hepatic sinusoids in control liver tissue. In cirrhotic liver (Child-A-LC and Child-C-LC), APJ expression was evident mainly along the sinusoids and on portal fibroblasts in fibrotic septa. Western blot analysis of whole-liver homogenate and LCM–PCR of sinusoids revealed overexpression of APJ in Child-C-LC samples. The results of IEM studies showed that APJ expression was increased significantly on HSCs, but it was sparse on SECs in Child-C-LC tissue. In vitro examination revealed that APJ was overexpressed in cultured HSCs activated by platelet-derived growth factor-β.
Conclusions Enhanced expression of APJ on HSCs in cirrhosis indicates markedly increased vascular remodeling.

Keywords Liver cirrhosis · Apelin receptor · Vascular remodeling

Electronic supplementary material The online version of this article (doi:10.1007/s00535-010-0296-3) contains supplementary material, which is available to authorized users.

H. Yokomori (✉) · F. Kaneko
Department of Internal Medicine, Kitasato Institute Medical Center Hospital, Kitasato University, 6-100 Arai, Kitamoto, Saitama 364-8501, Japan
e-mail: yokomori@insti.kitasato-u.ac.jp

M. Oda
Organized Center of Clinical Medicine, International University of Health and Welfare, Tokyo, Japan

K. Yoshimura
Department of Rehabilitation, Nihon Institute of Medical Science, Saitama, Japan

S. Machida
Biomedical Research Center, Saitama Medical University, Saitama, Japan

T. Hibi
Department of Internal Medicine, School of Medicine, Keio University, Tokyo, Japan

Introduction

Many orphan G protein-coupled receptors are regarded as specific receptors for unidentified hormones and neuropeptides [1]. A novel orphan G protein-coupled apelin receptor [APJ, a putative receptor protein related to the

angiotensin-type 1 receptor (AT1)/angiotensin-like-receptor 1 (AGTRL1)], was identified in a human gene [2]. A novel endogenous 36-amino-acid ligand for the APJ was named the apelin-36 peptide [3]. Apelin is expressed primarily in the endothelium. It acts both locally and via endocrine signaling to activate APJ. It is expressed on myocardial cells, endothelial cells, and some vascular smooth muscle cells [4–7]. Apelin, a newly identified angiotensin II homologue, has been shown to act as an endogenous ligand for the orphan receptor APJ; it counterbalances the actions of angiotensin II [8, 9]. Apelin peptides cause endothelium-dependent vasorelaxation by triggering the release of nitric oxide (NO). This effect can be abolished almost completely in the presence of an endothelial NO synthase (eNOS) inhibitor, N^G-nitro-L-arginine methyl ester (L-NAME), suggesting that apelin exerts a vasorelaxation effect via activation of the eNOS pathway [9, 10]. The circulation level of apelin was markedly higher in an experimental cirrhotic rat liver than it was in a control sample [11]. Apelin might also behave as a hepatic paracrine substance in the cirrhotic liver; it is secreted by activated stellate cells and interacts with neoangiogenic signaling pathways [10].

Little is known about the localization of APJ in the normal liver or its changes in the hepatic microvascular system, including the sinusoids in the cirrhotic liver. Moreover, results of in vitro and in vivo studies suggest that platelet-derived growth factor (PDGF) is the most potent mitogen of hepatic stellate cells (HSCs). It is therefore likely to be an important mediator of increased proliferation of HSCs during hepatic fibrogenesis in chronic liver diseases [12, 13]. In chronic hepatitis and cirrhosis, sinusoidal endothelial cells (SECs) frequently undergo transformation to a vascular type with the formation of a true basement membrane [14]. The in vivo formation of a capillary-like tubular network accompanying sinusoidal endothelial fenestral contraction in liver SECs (LSECs) can be demonstrated in vitro using Matrigel® (BD Bioscience, Franklin Lakes, NJ, USA) cultures and an SEC angiogenesis model, which shows endothelial cell migration and adhesion [15].

We attempted to clarify the localization of APJ in microvessels in normal and cirrhotic human liver tissues.

Materials and methods

Materials

As controls, wedge biopsy specimens of normal liver tissue were obtained from five patients (four male, one female; age 68–74 years, mean 72.0 years) who underwent surgical resection for metastatic liver carcinoma (all colon carcinomas). Cirrhotic liver specimens were obtained from gross cirrhotic portions that had been surgically resected from 10 patients (all male; age 66–72 years, mean 68.4 years) who had hepatocellular carcinoma (HCC) concurrent with hepatitis-C-related cirrhosis. All patients had undergone hepatectomy. All 10 patients had had a preoperative indocyanine green clearance test (ICG) value of <15%. They were evaluated as Child–Pugh grade A [16]. Informed consent for using resected tissue was obtained from all patients. Also, liver tissue specimens were obtained at autopsy from four patients who had had hepatitis-C-related Child–Pugh grade C cirrhosis (all male; ages 71–80 years, mean 74.6 years). All autopsies were performed within 3 h after death. Informed consent for autopsy was received in each case from the family of the deceased patient. The hospital ethics committee approved this study.

Immunoperoxidase staining

Liver tissues (approximately 3 cm × 2 cm × 1 cm) were fixed in formalin and embedded in paraffin. From the paraffin blocks, 4-μm sections were cut, deparaffinized with xylene, and dehydrated using graded ethanol. They were incubated overnight at 4°C with 1:200 dilution of anti-APJ rabbit polyclonal antibody (MBL International, Woburn, MA, USA). Then the sections were incubated using an Envision® system (Dako, Tokyo, Japan) at room temperature for 30 min. After repeated washing with phosphate buffered saline (PBS), the sections were reacted with diaminobenzidine containing 0.01% H_2O_2 and counterstained with hematoxylin for light microscopic study.

Computer-assisted morphometric analysis of APJ-labeled sinusoidal network

Sections immunohistochemically labeled with APJ were analyzed morphometrically. Briefly, the immunostained sections were scanned using light microscopy at low magnification (×40). The APJ immunostaining in sinusoidal lining cells was counted in a representative high-magnification (×400; 0.152 mm^2) field. Image analysis was done using a computer. Images were captured and digitized using an internal frame grabber board (Photoshop CS4/Photoshop CS4 Extended; Adobes Systems, Park Avenue, San Jose, CA, USA). This procedure consisted of converting the captured image into pixels. The number of APJ-immunostained sinusoidal lining cells per square millimeter was derived from image analyses [17]. Twenty fields containing hepatic sinusoids were measured for each control and cirrhotic liver tissue sample. Fisher's protected least significant difference (PLSD) test was used for statistical analysis.

Western blot

Liver samples were homogenized for 90 s in 10 volumes of homogenization buffer (20 mM Tris–HCl, pH 7.5; 5 mM $MgCl_2$; 0.1 mM phenylmethylsulfonyl fluoride (PMSF); 20 mM pepstatin A; and 20 μM leupeptin) using a Polytron (Vernon Hills, IL, USA) homogenizer at setting 7. The obtained membrane proteins were used for immunoblotting. Proteins (20 μg/mL) were separated using sodium dodecyl sulfate polyacrylamide gel electrophoresis (SDS-PAGE) and transferred onto polyvinylidene difluoride membranes (Life Sciences/Pall, Port Washington, NY, USA). The blots were blocked with 5% (w/v) dried milk in PBS for 30 min. Then they were incubated with anti-APJ (MBL International) diluted 1: 5000 in 0.1% Tween 20 in PBS. After rinsing in PBS, color was developed using an ECL® system (Super Signal West Femto; Pierce Biotechnology, Rockford, IL, USA). The bands were visualized using a diaminobenzidine solution containing 0.01% H_2O_2.

Laser capture microdissection

Liver tissues were frozen immediately in OCT compound (Sakura Finetechnical, Tokyo, Japan) and stored at −80°C until use. After rapid staining with toluidine blue, sinusoidal cells in 6-μm frozen sections were microdissected using a laser microdissection system (Palm laser; Palm Microlaser Technologies, Bernried, Germany). Briefly, a specific polymer film mounted on optically transparent caps (Palm Microlaser Technologies) was placed on the section. Sinusoidal cells were captured by focal melting of membranes using the laser beam under visual control [18, 19]. The caps with captured epithelial cells were used as lids for 500-μL microcentrifuge tubes containing RNA extraction buffer (Arcturus Engineering, Sunnyvale, CA, USA).

RNA extraction and reverse transcription polymerase chain reaction (RT-PCR)

Total RNA was extracted from each laser capture microdissection (LCM) sample using TRIzol RNA isolation reagent (Life Technologies, Tokyo, Japan) according to the manufacturer's recommendations. After processing, the dried pellet was resuspended in RNase-free sterile water (Nippon Gene, Toyama, Japan). Then RNA from each sample was reverse-transcribed into cDNA using a cDNA synthesis kit (PrimeScript II 1st strand; TaKaRa Holdings, Shiga, Japan). The RT step was performed in a reaction volume of 20 μL according to the manufacturer's instructions, but using approximately 1 μg of total RNA from each sample. The reaction mixtures were incubated at 42°C for 60 min and then heated to 95°C for 5 min. The cDNA was used directly for PCR. The primers, which target chromosome 11, were the following: sense primer 5′-CC TTGTGGTTGACTAGGGCTGG and antisense primer 5′-GGCTTGTGCAGGGTCAGGTCT. Amplification was performed using polymerase (TaKaRa EX Taq; TaKaRa Holdings) and 3 μL of cDNA, with the following protocol: 40 cycles of 30 s at 94°C, 30 s at 58°C, and 1 min at 72°C, combined with final extension of 7 min. Control primer sequences were the following: glyceraldehyde-3-phosphate-dehydrogenase (GAPDH) primer, 5′-CGGGAA ATCGTG CGTGAC-3′, and 5′-CAG GTC TTT GCG GAT GTC CAC-3′.

Immunogold–silver staining method for electron microscopy

Liver tissues were fixed in periodate-lysine-paraformaldehyde (PLP). Semithin 5 μm sections were immersed for 15 min in three changes of 0.01% PBS (pH 7.4). They were then incubated with anti-APJ rabbit polyclonal antibody diluted 1: 200 in 0.01 M PBS containing 1% bovine serum albumin) overnight at 4°C in a moisture chamber. Subsequently, they were treated for 15 min in PBS three times, incubated in 1.4-nm colloidal gold-conjugated anti-rabbit IgG antibody (1: 50 dilution; Nanoprobes, Yaphank, NY, USA) for 40 min, and physically developed using a silver enhancement kit (Nanoprobe Silver Enhancement Kit; Nanoprobes) [20]. For transmission electron microscopy, the materials were treated for 15 min in PBS three times and fixed in 1.2% glutaraldehyde buffered with 0.01% phosphate buffer (pH 7.4) for 1 h at 4°C, followed by treatment with a graded series of ethanol solutions and postfixation with 1% osmium tetroxide in 0.01% phosphate buffer (pH 7.4). After embedding in Epon, ultrathin sections were cut with a diamond knife on an LKB (Bromma, Sweden) ultramicrotome, stained with uranyl acetate, and observed under a transmission electron microscope (TEM; JEM-1200 EX; JEOL, Tokyo, Japan) at 80 kV acceleration voltage.

The immunogold labeling of perisinusoidal SECs in ultrathin sections was semi-quantitated using image analysis software (Mac Measure Program, NIH Image ver. 1.62; National Institutes of Health [NIH], Bethesda, MD, USA). The SECs around sinusoids (×4000) were selected randomly, and the gold particles per unit length of membrane were counted ($n = 19$).

Statistical analysis

Data are expressed as means ± SEM. For Western blot analysis and LCM coupled with RT-PCR, the relative expression of APJ was determined using densitometric scanning (image J; NIH). Statistically significant differences between means were determined using one-way analysis of variance (ANOVA) on ranks, followed by an all

pairwise multiple comparison procedure (Fisher's PLSD test), as appropriate. For immunogold labeling of HSCs and SECs in ultrathin sections, the statistical significance of differences in the number of gold particles per unit length of membrane between control and cirrhotic samples was analyzed using Student's *t*-test. A *p* value of less than 0.05 was inferred as indicating a significant difference.

In vitro study

We explored the role of the HSC as a liver-specific pericyte and the SEC as a capillary endothelial cell with angiogenic properties that contribute to sinusoidal remodeling in the liver.

Both human HSCs and primary human SECs (ScienCell Research Laboratories, Carlsbad, CA, USA) were used between passages 3 and 6. The HSCs and SECs were cultured in defined medium (ScienCell Research Laboratories) supplemented with 10% fetal bovine serum (where indicated), L-glutamine (1 mmol/L), penicillin (100 IU/mL), and streptomycin (100 μg/mL). The SECs were seeded on Matrigel®-coated or collagen-coated cover glasses (Biocoat 4426; Becton–Dickinson, BD Bioscience) placed in two-well dishes (Falcon 3001; BD Falcon, Lincoln Park, NJ, USA), and incubated with or without vascular endothelial growth factor (VEGF) (0.1–2 ng/mL) in a CO_2 gas incubator at 37°C for 24 h. The HSCs were seeded on collagen-coated cover glasses (Biocoat 4426; Becton–Dickinson), placed in six-well (Falcon 3046; BD Falcon) or two-well dishes (Falcon 3001; BD Falcon), and exposed to platelet-derived growth factor (PDGF)-BB (0.1–2 ng/mL) and/or the PDGF receptor inhibitor imatinib (0.1–2 μmol/L) for 24 h.

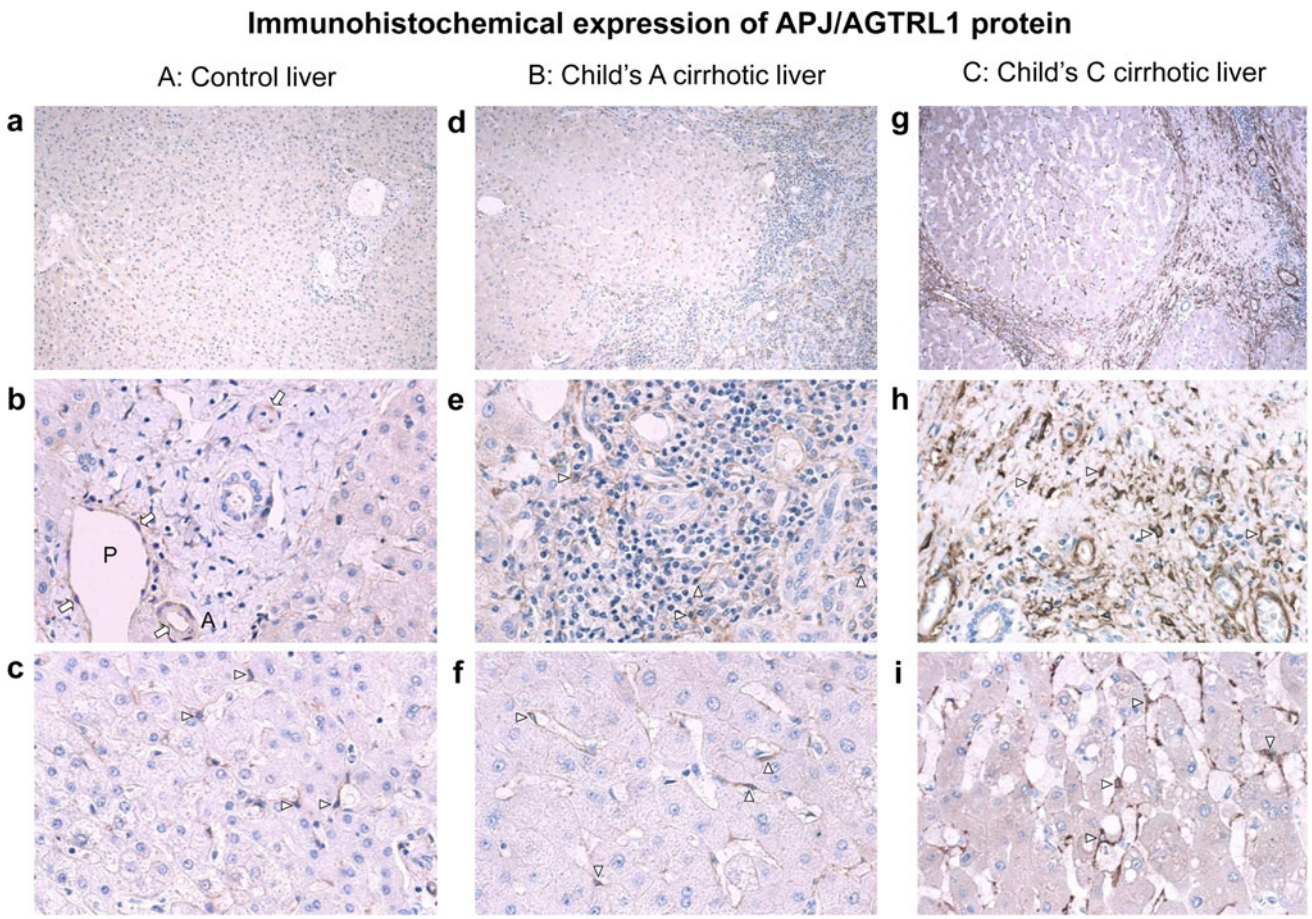

Fig. 1 **A** Immunohistochemical distribution of apelin receptor (*APJ*) in human control liver (**A**: *a–c*), Child-A cirrhotic liver (**B**: *d–f*), and Child-C cirrhotic liver (**C**: *g–i*), using immunoperoxidase staining with hematoxylin counterstain. *Arrows* indicate the hepatic artery and portal vein; *arrowheads* indicate a sinusoidal lining cell; *P* denotes portal vein. **A** Control liver tissue. Immunohistochemistry revealed APJ expression on the vascular smooth muscle layers of the hepatic artery (*A*) and portal vein (*P*) in the portal tract (*a*, *b*), but APJ is visible only sparsely in hepatic sinusoidal lining cells (*a*, *c*). **B** Child-A liver tissue. In early-stage cirrhotic liver, APJ is evident mainly at the sites of sinusoidal lining cells in regions of nodules (*d–f*). Myofibroblast-like spindle-shaped cells also show APJ immunopositive reactivity that is more intense in the fibrous septum (*d*, *f*). **C** Child-C liver tissue. In the late-stage cirrhotic liver, intense APJ immunoreactivity is visible mainly on sinusoidal lining cells in the regenerating nodules and in the peripheral regions of nodules and fibrous septa. It is more intense in severely fibrotic tissues and pericytes around the terminal and sublobular hepatic veins (*g–i*) than in the Child-A cirrhotic liver (*d–f*). *AGTRL1* Angiotensin-like-receptor 1 (*a*, *d*, *g* ×100; *b*, *c*, *e*, *f*, *h*, *i* ×400)

After culture, the HSCs and SECs were lysed and prepared for Western blot analysis as described above. We specifically investigated the expression of APJ or GAPDH.

Results

In vivo immunohistochemistry

In control liver tissue, APJ was mainly localized in the aortic artery and portal vein, although APJ was also detected, only slightly, in the sinusoids (Fig. 1A-a, b, c). In Child-A cirrhotic tissue, APJ was observed mainly at the sites of sinusoidal lining cells in the regions of nodules, in arterial capillaries in fibrotic septum at the periphery of the nodule in severely fibrotic tissues (Fig. 1B-d, e, f). In Child-C liver tissue, intense APJ immunoreactivity was detected mainly on sinusoidal lining cells in the regenerating nodules and in the peripheral regions of nodules and fibrous septa. It was more intense in severely fibrotic tissues and pericytes around the terminal and sublobular hepatic veins than in Child-A LC (Fig. 1C-g, h, i). Using morphometric measurements, we found that APJ immunostaining was 2.043 pixels/mm^3 in control, 4.427 pixels/mm^3 in Child A liver cirrhosis, and 8.074 pixels/mm^3 in Child C liver cirrhosis. The immunostaining was significantly higher in Child C than in Child A ($p < 0.001$) or control ($p < 0.001$) tissues. Moreover, it was significantly higher in the control sample than in Child A liver cirrhosis ($p < 0.001$) (Fig. 2).

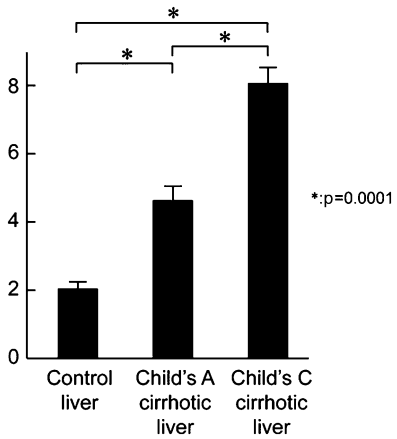

Fig. 2 Computer-assisted morphometric analysis of APJ-labeled sinusoidal network. *PLSD* (Fisher's) protected least significant difference, *ANOVA* analysis of variance

To confirm the immunohistochemical results, we investigated the protein expression of APJ in normal and cirrhotic liver tissues using Western blot analysis. The APJ protein was expressed more abundantly in Child-C cirrhotic liver tissue than in either the control or the Child-A tissues (Fig. 3).

RT-PCR

The APJ mRNA levels in hepatic sinusoids in Child-C cirrhotic liver samples were significantly higher than in those in either the control or the Child-A samples (Fig. 4d).

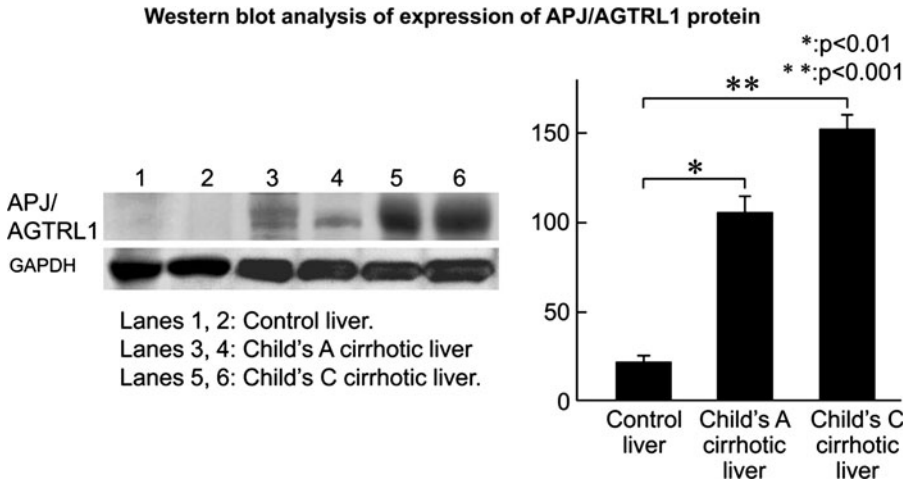

Fig. 3 Western blot analysis of APJ protein expression in human control and cirrhotic liver tissues. Samples containing 20 μg protein were subjected to sodium dodecyl sulfate polyacrylamide gel electrophoresis (SDS-PAGE) and analyzed using Western blotting. *Lanes 1 and 2* control liver tissues, *lanes 3 and 4* Child-A cirrhotic liver, *lanes 5 and 6* Child-C cirrhotic liver. Positions of molecular mass markers (kDa) are shown. APJ protein expression is markedly enhanced in Child-C cirrhotic liver. *GAPDH* Glyceraldehyde-3-phosphate-dehydrogenase

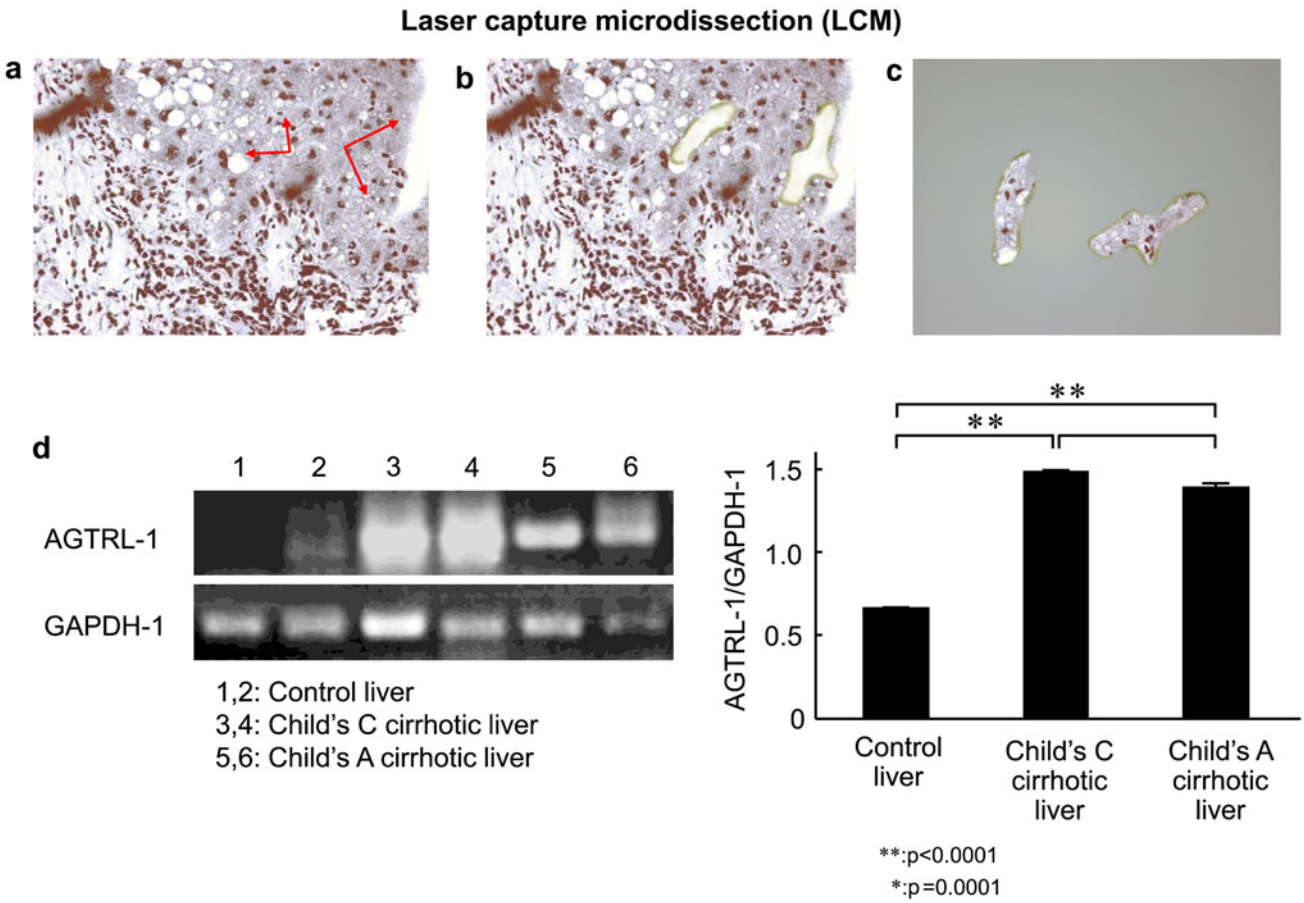

Fig. 4 Laser-capture microdissection (*LCM*) coupled with reverse transcription polymerase chain reaction (RT-PCR) for fresh-frozen sections of liver tissue stained with toluidine blue (original magnification ×200). **a** Liver tissue sample before removal of the target sinusoidal cells using LCM. **b** Child-C cirrhotic liver tissue sample after removal of the sinusoidal cells using LCM. **c** LCM-captured sinusoidal cells attached to transfer film. **d** The *APJ* mRNA level from liver parenchyma is significantly higher in Child-C LC samples than in either control or Child-A LC samples. Gel photograph of PCR for GAPDH and APJ showing PCR products of the expected sizes

Immunogold–silver enhancement

Next, we examined the ultrastructural localization of APJ on sinusoidal lining cells, using immunogold electron microscopy. In control liver tissues, electron-dense gold particles showing the presence of APJ were scarcely found on HSCs and LSECs. They were mainly localized on the luminal side (Fig. 5a). Child-A cirrhotic liver tissues showed slightly more APJ, not only on HSCs but also on LSECs (Fig. 5b), compared to control liver tissues. Child-C cirrhotic liver tissues showed significantly more APJ on HSCs but similarly low expression on SECs, compared to control liver and Child-A cirrhotic liver tissues (Fig. 5c). In the fibrotic septum of Child C cirrhotic tissue, increased APJ expression was observed on myofibroblastic cells and fibroblasts, but sparsely on capillary endothelial cells (Fig. 5d).

Morphometric analysis of immunogold particle labeling for APJ (Fig. 5e) showed that APJ labeling was extremely low on HSCs in both control and Child-A cirrhotic liver tissues, but was significantly higher on HSCs in Child-C cirrhotic liver tissues: LSECs (control $3.0 \pm 0.2/2$ μm; Child-A 2.4 ± 0.2, not significant; Child C 3.1 ± 0.3, not significant) and HSCs (control 4.6 ± 0.2; Child-A 7.3 ± 0.2, $p < 0.01$; Child-C 20.2 ± 0.3, $p < 0.001$).

In vitro study

We next assessed whether human HSCs expressed APJ when stimulated by PDGF. In HSCs cultured with PDGF, APJ expression was detected, but it was not detected in HSCs that had been cultured with imatinib plus PDGF (Fig. 6A, B). This finding suggests that PDGF is involved in the overexpression of APJ in human HSCs. In another in vitro study, APJ was also overexpressed in HSCs cocultured with proinflammatory and contractility-related cytokines such as transforming growth factor-β, tumor necrosis factor-α, and endothelin-1 (supplemental data).

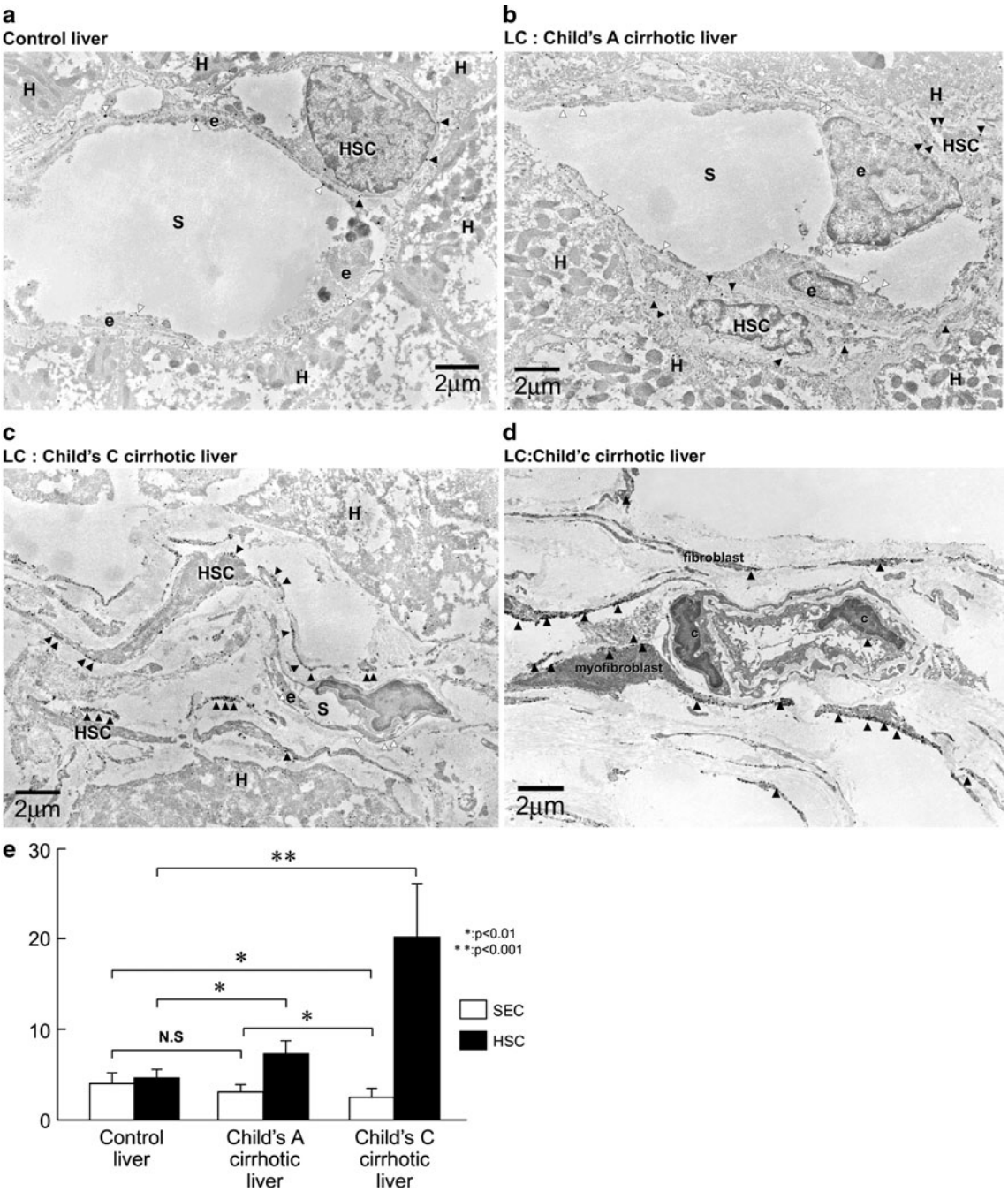

Fig. 5 Ultrastructural localization of APJ using immunogold electron microscopy in human control liver (**a**), Child-A cirrhotic liver (**b**), Child-C cirrhotic liver (**c**), and fibrotic septum of Child-C cirrhotic liver tissue (**d**). **a** Control liver tissue. Immunospecific particles, showing the presence of APJ, are observed sparsely on hepatic stellate cells (*HSC*s) and sinusoidal endothelial cells (SECs) in control liver tissue. **b** Child-A cirrhotic liver tissue. Immunospecific particles, showing the presence of APJ, are significantly more numerous on HSCs/myofibroblastic cells (MFs), but are also present on SECs. **c** Child-C cirrhotic liver tissue. APJ-positive particles are markedly increased on HSCs/MFs, as well as on their thin and elongated cytoplasmic processes in the widened space of Disse. However, these particles are scarce on SECs. Electron micrographs of cells stained with uranyl acetate. *Arrowheads* indicate APJ labeled with gold and silver particles. **d** Fibrotic septum of Child-C cirrhotic liver tissue. APJ-positive particles are markedly increased on myofibroblastic cells and fibroblasts, but scarce on capillary endothelial cells. **e** Morphometric analysis of immunogold particle labeling for APJ. The APJ labeling is extremely low on HSCs both in control and Child-A cirrhotic liver tissues, but is significantly higher on HSCs in Child-C cirrhotic liver tissues. *e* SEC, *HSC* hepatic stellate cell, *H* hepatocytes, *c* capillary endothelial cell, *S* hepatic sinusoid, *N.S* not significant. *Bar* 2 μm

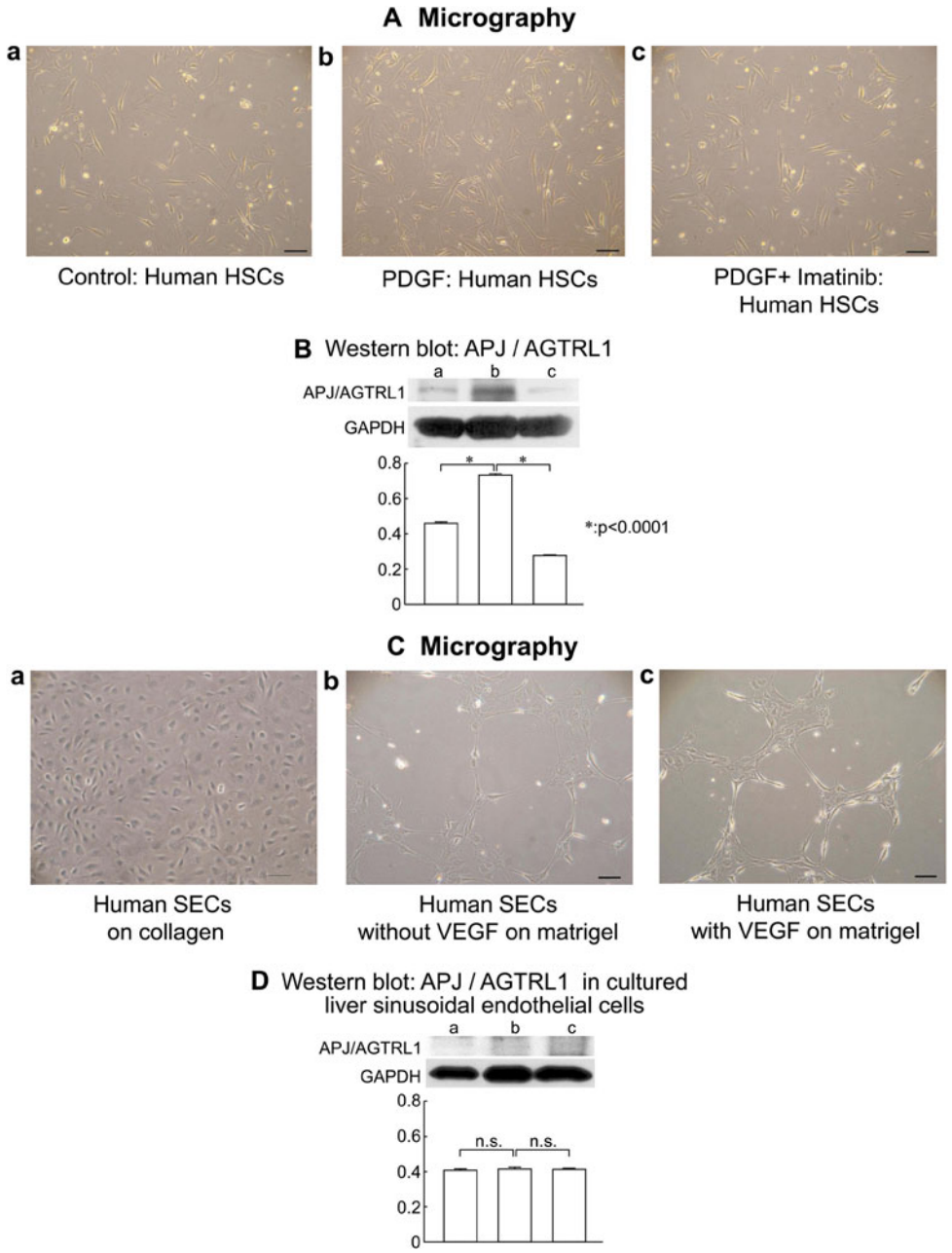

Fig. 6 Microscopic analysis and Western blots of in vitro expression of APJ on human HSCs and SECs. **A** Phase-contrast micrographs (×100) of human HSCs. *a* Human HSCs cultured on collagen without platelet-derived growth factor (PDGF). *b* Human HSCs (HHSCs) cultured on collagen with PDGF. The sizes and numbers of HHSCs are increased. *c* Human HSCs cultured on collagen with PDGF plus imatinib. **B** Western blots of APJ in HHSCs. *Lane a* 24 h culture on collagen without PDGF. *Lane b* 24 h culture on collagen with PDGF. *Lane c* 24 h culture on collagen with PDGF plus imatinib. The APJ protein level is much higher in HSCs cultured with PDGF than in those cultured without PDGF, or in those cultured with PDGF plus imatinib. *Upper panel* APJ. *Lower panel* GAPDH. **C** Phase-contrast micrographs (×100) of human SECs cultured on a collagen-coated or Matrigel®-coated dish. *a* Human SECs cultured on collagen without vascular endothelial growth factor (VEGF) for 24 h. Cells spread with a cobblestone-like appearance. *b* Human SECs cultured on Matrigel® without VEGF for 24 h. Cells became mostly connected. *c* Human SECs cultured on Matrigel® for 24 h, then for another 17 h in the presence of 10 ng/mL VEGF. Migration of liver SECs (LSECs) and capillary-like tube formation with multiple cell–cell connections are observed. **D** Western blots of APJ in human SECs (HSECs). Samples containing 30 μg of protein were subjected to SDS-PAGE (4–20% gels) and analyzed using Western blotting. *Lane a* 24 h culture on collagen without VEGF. *Lane b* 24 h culture on Matrigel® without VEGF. *Lane c* 24 h culture on Matrigel® with VEGF. VEGF protein expression level in HSECs is almost identical in all lanes. *n.s.*, Not significant

The direct effect of VEGF-stimulated capillary formation by LSECs on APJ expression was examined (Fig. 6C). The SECs were cultured for 24 h on a collagen-coated or Matrigel®-coated cover glass with or without VEGF. APJ was expressed sparsely on SECs plated on collagen or on Matrigel in the presence or absence of VEGF, with no significant difference (Fig. 6D).

Discussion

Apelin is a recently described endogenous peptide that plays an important role in heart physiology and pathophysiology. Apelin has in vivo inotropic effects on normal and failing hearts [4] and on angiogenesis [10]. Apelin can act directly on APJ within vascular smooth muscle to induce contraction, but this effect is outweighed by stimulation of local nitric oxide production via endothelial APJ in the presence of functioning endothelium [10]. Apelin might also behave as a hepatic paracrine substance in the cirrhotic liver, secreted by activated stellate cells interacting with multiple signaling pathways [10].

No data related to the in vivo pattern of APJ expression in hepatic sinusoidal cells have been reported, either in normal human liver or in liver affected by chronic liver disease. In the present study, immunohistochemical staining of APJ was found on sinusoidal lining cells throughout the hepatic parenchyma at high magnification, especially in Child C cirrhotic liver. Moreover, positive staining of pericytes was observed around the terminal and sublobular hepatic veins. Portal areas showed strong positivity around the bile ducts and in the arterial tunica media, with moderate positivity in the walls of portal veins, especially in Child C cirrhotic tissue. Morphometric analysis based on APJ immunostaining of hepatic sinusoidal cells confirmed that APJ expression was significantly and prominently higher in the end-stage than in the mild cirrhotic stage. The extent of APJ protein expression in control and cirrhotic liver samples was confirmed using Western blot analysis. To study APJ expression at the RNA level in hepatic sinusoidal cells, we used LCM to isolate sinusoidal lining cells, comprising HSCs and SECs. In fact, LCM technology can harvest the cells of interest directly or can isolate specific cells by cutting away unwanted cells to produce histologically pure or enriched cell populations [19]. When RT-PCR was performed on the isolated sinusoidal cells, it revealed significantly higher *APJ* mRNA expression in cirrhotic liver than in the control sample. This report is the first to describe the expression of APJ at the protein level in whole liver and at the mRNA level in hepatic sinusoids in cirrhotic and normal liver tissues, suggesting higher secretion of APJ in hepatic sinusoids of cirrhotic liver.

Our immunogold electron microscopy of human liver tissue revealed some ultrastructural expression of APJ on the HSCs and SECs detected in the control liver. In contrast, APJ was strongly expressed on the HSCs in Child-C liver tissue. In the fibrotic septum, APJ expression was observed on myofibroblastic cells and fibroblasts. In the presence of intact endothelium, the net effect of APJ expression is vasodilatation. In cirrhosis, especially in Child C decompensated cirrhosis, apelin can act directly on APJ within HSCs to induce contraction, but in the presence of functioning SECs, this effect is outweighed by decreased local NO production via APJ in SECs [5]. The results of the present study suggest that enhanced APJ expression in advanced cirrhosis might intensify the effect of apelin on HSCs to increase hepatic microvascular tone. In addition, the marked overexpression of APJ might be associated with the phenotypic activation of human HSCs into myofibroblasts and portal myofibroblasts.

Several substances involved in hepatic wound healing, in particular PDGF and endothelin-1, stimulate angiotensin II synthesis by activated HSCs [21, 22]. The results of the present in vitro study suggest that apelin contributes to the PDGF-induced proliferation of HSCs. In fact, HSCs are also regarded as liver-specific pericytes, but their role in modulating angiogenesis, particularly in pathological conditions, might differ substantially from the role attributed to microcapillary pericytes [23]. In the present study, APJ was sparsely detected on the capillary-like tube formations of hepatic SECs after plating on Matrigel in the presence or absence of VEGF. In a previous study, the expression of APJ was high in the retinal endothelial cell line RF/6F, but it was almost negligible in human umbilical endothelial cells [24]. Therefore, APJ expression in capillary endothelial cells might be unique, which might account for the low APJ protein expression in SECs observed in our vitro study and confirmed by the immunoelectron microscopic (IEM) findings in our vivo study.

The apelin antagonist F13A significantly ameliorated fibrosis-associated neoangiogenesis in cirrhotic rats with ascites [11]. In fact, F13A abolished the apelin-induced blood pressure-lowering effect in vivo in hypertensive animals [24, 25]. It effectively reduced splanchnic neovascularization in portal hypertensive rats, and markedly decreased apelin-induced vascular smooth muscle contraction [10, 26]. Moreover, the angiogenic activity is the consequence of apelin action on the proliferation and migration of endothelial cells. Apelin activates the cell transduction cascades (ERKs, Akt, and p70S6kinase phosphorylation) [27] leading to the proliferation of endothelial cells and the formation of new blood vessels [23]. Apelin also stimulates myosin-light chain phosphorylation in rat and mouse vascular smooth muscle [10, 26]. In capillarized sinusoidal endothelium, apelin can act

directly on APJ receptors within HSCs or myofibroblastic cells to induce contraction. Consequently, apelin signaling represents a new and interesting therapeutic target during pathological neovascularization associated with portal hypertension [24].

In summary, we report for the first time that APJ expression at the protein and RNA levels is markedly increased in the sinusoid lining cells of human cirrhotic liver, and that APJ is overexpressed in activated HSCs in sinusoids as well as in myofibroblasts and in fibroblasts in fibrotic septa in Child-C cirrhosis. The present results suggest that APJ plays a role in vascular remodeling and in increased portal hypertension in cirrhosis. In HSCs activated by PDGF and proinflammatory cytokines in our in vitro study, APJ was overexpressed, suggesting that APJ might contribute to the proinflammatory cytokine-stimulated proliferation of HSCs in fibrogenesis. Both our in vivo and in vitro studies have shown that APJ is weakly expressed in SECs.

Acknowledgments We appreciate technical advice from Kumiko Komatsu and Masumi Akita (Division of Morphological Science, Biomedical Research Center, Saitama Medical School).

References

1. Chung S, Funakoshi T, Civelli O. Orphan PCR research. Br J Pharmacol. 2008;153(Suppl 1):S339–46.
2. O'Dowd BF, Heiber M, Chan A, Heng HH, Tsui LC, Kennedy JL, et al. A human gene that shows identity with the gene encoding the angiotensin receptor is located on chromosome 11. Gene. 1993;136:355–60.
3. Tatemoto K, Hosoya M, Habata Y, Fujii R, Kakegawa T, Zou MX, et al. Isolation and characterization of a novel endogenous peptide ligand for the human APJ receptor. Biochem Biophys Res Commun. 1998;251:471–6.
4. Chen MM, Ashley EA, Deng DX, Tsalenko A, Deng A, Tabibiazar R, et al. A novel role for the potent endogenous inotrope apelin in human cardiac dysfunction. Circulation. 2003;108:1432–9.
5. Kleinz MJ, Davenport AP. Immunocytochemical localization of the endogenous vasoactive peptide apelin to human vascular and endocardial endothelial cells. Regul Pept. 2004;118:119–25.
6. Kleinz MJ, Skepper JN, Davenport AP. Immunocytochemical localisation of the apelin receptor, APJ, to human cardiomyocytes, vascular smooth muscle and endothelial cells. Regul Pept. 2005;126:233–40.
7. Sheikh AY, Chun HJ, Glassford AJ, Kundu RK, Kutschka I, Ardigo D, et al. In vivo genetic profiling and cellular localization of apelin reveals a hypoxia-sensitive, endothelial-centered pathway activated in ischemic heart failure. Am J Physiol Heart Circ Physiol. 2008;294:H88–98.
8. Ishida J, Hashimoto T, Hashimoto Y, Nishiwaki S, Iguchi T, Harada S, et al. Regulatory roles for APJ, a seven-transmembrane receptor related to angiotensin-type 1 receptor in blood pressure in vivo. J Biol Chem. 2004;279:26274–9.
9. Ashley E, Chun HJ, Quertermous T. Opposing cardiovascular roles for the angiotensin and apelin signaling pathways. J Mol Cell Cardiol. 2006;41:778–81.
10. Japp AG, Newby DE. The apelin-APJ system in heart failure: pathophysiologic relevance and therapeutic potential. Biochem Pharmacol. 2008;75:1882–92.
11. Principe A, Melgar-Lesmes P, Fernández-Varo G, Del Arbol LR, Ros J, Morales-Ruiz M, et al. The hepatic apelin system: a new therapeutic target for liver disease. Hepatology. 2008;48:1193–201.
12. Mancini R, Jezequel AM, Benedetti A, Paolucci F, Trozzi L, Orlandi F. Quantitative analysis of proliferating sinusoidal cells in dimethylnitrosamine-induced cirrhosis. An immunohistochemical study. J Hepatol. 1992;15:361–6.
13. Pinzani M, Gesualdo L, Sabbah GM, Abboud HE. Effects of platelet derived growth factor and other polypeptide mitogens on DNA synthesis and growth of cultured rat liver fat-storing cells. J Clin Invest. 1989;84:1786–93.
14. Fukuda Y, Nagura H, Imoto M, Koyama Y. Immunohistochemical studies of structural changes of the hepatic lobules in chronic liver diseases. Am J Gastroenterol. 1986;81:1149–55.
15. Yokomori H, Oda M, Yoshimura K, Nagai T, Fujimaki K, Watanabe S, et al. Caveolin-1 and Rac regulate endothelial capillary-like tubular formation and fenestral contraction in sinusoidal endothelial cells. Liver Int. 2009;29:266–76.
16. Lam CM, Fan ST, Lo CM, Wong J. Major hepatectomy for hepatocellular carcinoma in patients with an unsatisfactory indocyanine green clearance test. Br J Surg. 1999;86:1012–7.
17. Hamilton PW, Allen DC. Morphometry in histopathology. J Pathol. 1995;175:369–79.
18. Schutze K, Posl H, Lahr G. Laser micromanipulation systems as universal tools in cellular and molecular biology and in medicine. Cell Mol Biol (Noisy-le-grand). 1998;44:735–46.
19. Emmert-Buck MR, Bonner RF, Smith PD, Chuaqui RF, Zhuang Z, Goldstein SR, et al. Laser capture microdissection. Science. 1996;274:998–1001.
20. Humbel BM, Sibon OC, Stierhof Y-D, Schwarz H. Ultra-small gold particles and silver enhancement as a detection system in immunolabeling and in situ hybridization. J Histochem Cytochem. 1995;43:735–7.
21. Bataller R, Sancho-Bru P, Ginès P, Lora JM, Al-Garawi A, Solé M, et al. Activated human hepatic stellate cells express the renin-angiotensin system and synthesize angiotensin II. Gastroenterology. 2003;125:117–25.
22. Lindahl P, Johansson BR, Leveen P, Betsholtz C. Pericyte loss and microaneurysm formation in PDGF-B-deficient mice. Science. 1997;277:242–5.
23. Kasai A, Shintani N, Oda M, Kakuda M, Hashimoto H, Matsuda T, et al. Apelin is a novel angiogenic factor in retinal endothelial cells. Biochem Biophys Res Commun. 2004;325:395–400.
24. Sorli SC, Van den Berghe L, Masri B, Knibiehler B, Audigier Y. Therapeutic potential of interfering with apelin signalling. Drug Discov Today. 2006;11:1100–6.
25. Hashimoto T, Kihara M, Ishida J, Imai N, Yoshida S, Toya Y, et al. Apelin stimulates myosin light chain phosphorylation in vascular smooth muscle cells. Arterioscler Thromb Vasc Biol. 2006;26:1267–72.
26. Tiani C, Garcia-Pras E, Mejias M, de Gottardi A, Berzigotti A, Bosch J, et al. Apelin signaling modulates splanchnic angiogenesis and portosystemic collateral vessel formation in rats with portal hypertension. J Hepatol. 2009;50:296–305.
27. Masri B, Lahlou H, Mazarguil H, Knibiehler B, Audigier Y. Apelin (65–77) activates extracellular signal-regulated kinases via a PTX-sensitive G protein. Biochem Biophys Res Commun. 2002;290:539–45.